Magnus-Based Airborne Wind Energy Systems

Yashank Gupta ,Jonathan Dumon, Ahmad Hably
yashank.gupta@gipsa-lab.fr
jonathan.dumon@gipsa-lab.fr
ahmad.hably@gipsa-lab.fr

Introduction

Among the Airborne Wind Energy concepts Magnus based airborne wind energy systems uses rotating cylinders as aerostat. The rotating cylinder when exposed to wind flow produces a lift force, described as Magnus effect. The Magnus based aerostat have a high lift coefficient which is supplemented by lighter than air capabilities, and have a naturally robust design. The aerostat following a predefined trajectory leads to the development of high traction force in the tether which in turn is used to drive the generator and produce electricity.

Magnus Effect

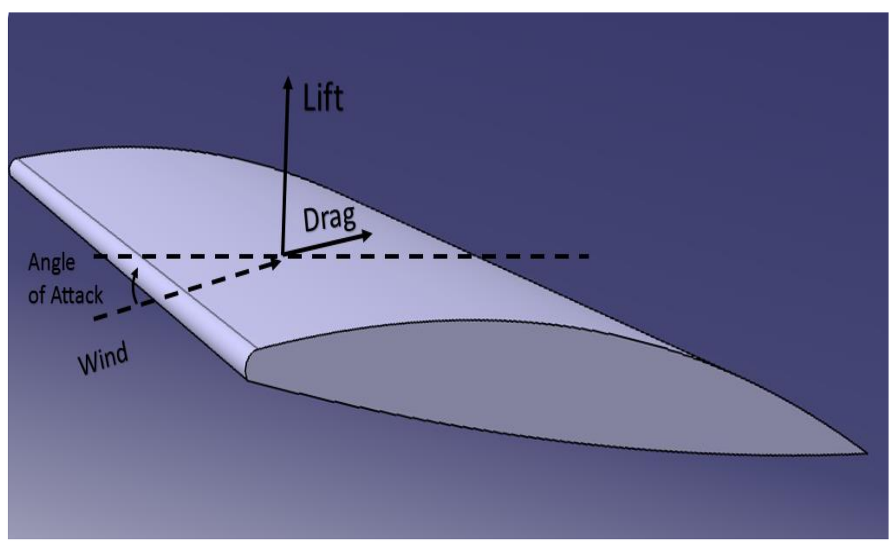

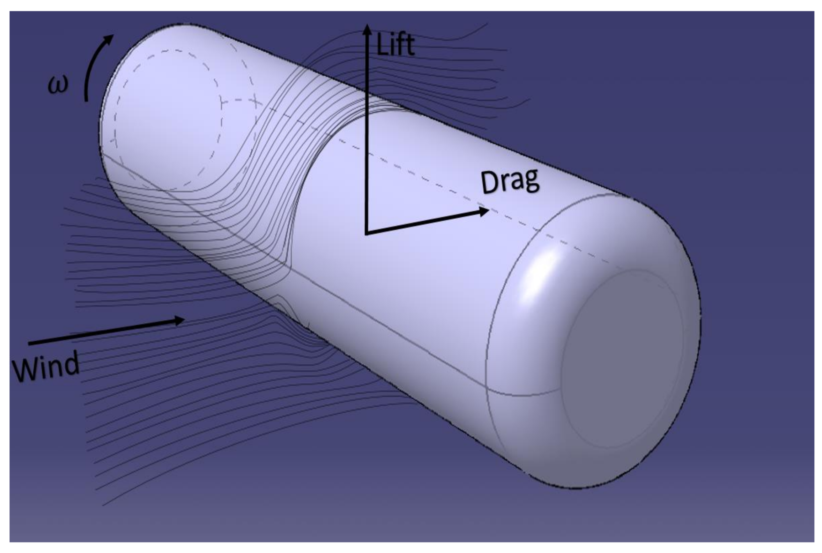

C_L: Coeff. of Lift, C_D: Coeff. of Drag, X : *Spin ratio* $= \frac{\omega_{cyl} r_{cyl}}{v_{axz}}$, C_{Dy}: Coeff. of Drag-y_b $-$ *direction*

F_L : *Lift Force* $= \frac{1}{2}\rho S_{cyl} v_{axz}^2 C_L$, F_D : *Drag Force* $= \frac{1}{2}\rho S_{cyl} v_{axz}^2 C_D$,

F_{D_y} : *Drag Force* $, y_b -$ *direction* $= \dfrac{1}{2}\rho S_{cyl} v_{ay}^2 C_{Dy}$

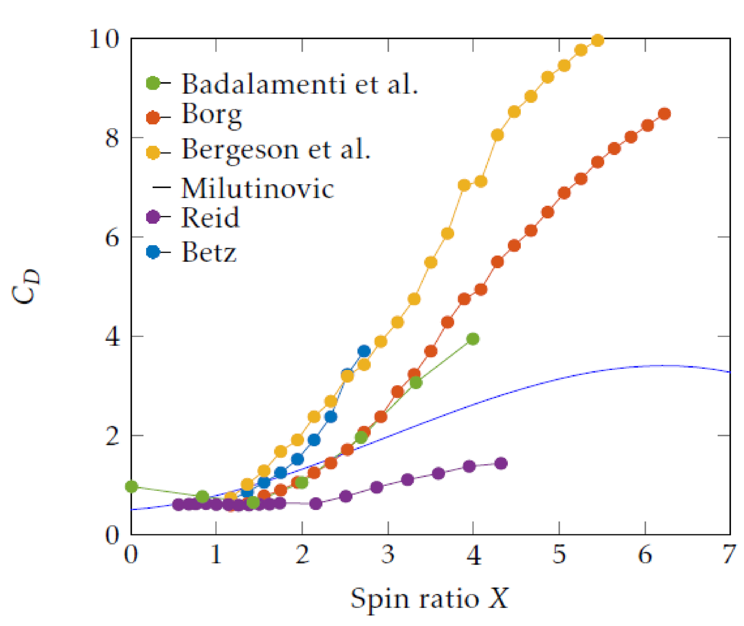

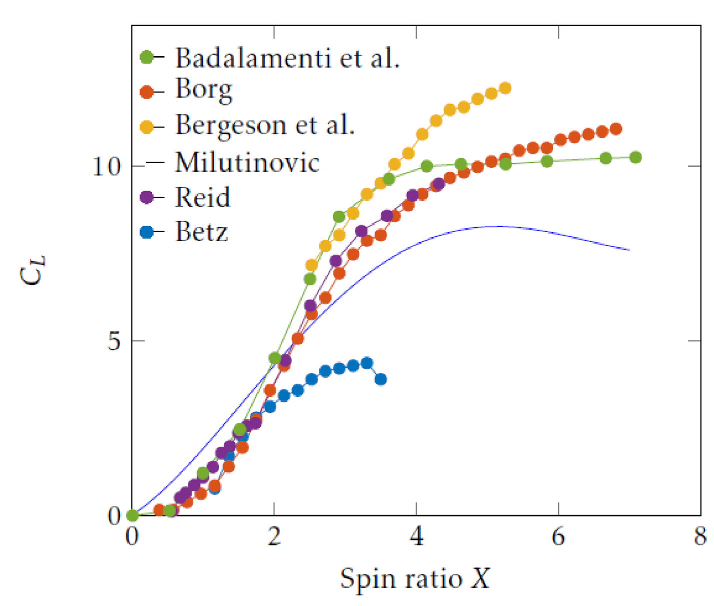

The above analysis shows that the assumed polynomial expressions for the Coeff. of Lift (C_L) and the Coeff. of Drag (C_D) .i.e. the aerodynamic model for Magnus cylinder as proposed by Miltuiovnic [1] agrees with the historical experimental data available on Magnus cylinder.

$$C_D = -0.0211X^3 + 0.1873X^2 + 0.1183X + 0.5,$$
$$C_L = 0.0126X^4 - 0.2004X^3 + 0.7482X^2 + 1.3447X$$

Mathematical Model

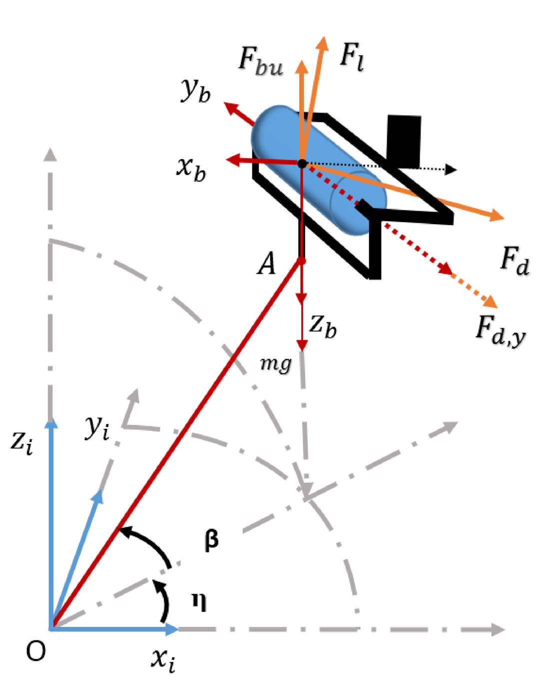

Equation of rate of change of translational velocity [2]

$$\dot{\mathbf{v}}_\mathbf{b} = \frac{\mathbf{1}}{\mathbf{m}}(\mathbf{F_b} - \widetilde{\boldsymbol{\omega}}_\mathbf{b}\, \mathbf{v_b})$$

where,

$$\widetilde{\omega}_b = \begin{bmatrix} 1 & -r & q \\ r & 0 & -p \\ -q & p & 0 \end{bmatrix}, \text{ and}$$

F_b represents Body forces acting on the ABM and is given by

$$\mathbf{F_b = F_L + F_D + F_{dy} + W_b + F_{bu} + F_r}$$

$\boldsymbol{W_b}$: Weight in Body Frame,
$\mathbf{F_{bu}}$: Bouyant Force,
$\boldsymbol{F_r}$: Rope Force,
$\{\boldsymbol{x_b - y_b - z_b}\}$: Body frame of ref. ,
$\{\boldsymbol{x_i - y_i - z_i}\}$: Inertial frame of ref.

$\boldsymbol{p}$: Roll rate,
$\boldsymbol{q}$: Pitch Rate,
$\boldsymbol{r}$: Yaw Rate,
$\boldsymbol{\beta}$: Elevation angle,
$\boldsymbol{\eta}$: Azimuthal angle

Static Model

- **Theoretical Power produced during production phase ($\boldsymbol{P_{prod}}$) as proposed by [3] Loyd (1980) and refined in [4] Argatov et al. (2009)**

  $P_{prod} = \frac{1}{2}\rho 4 S_{cyl}\left(\frac{v_\omega \cos(\beta)}{3}\right)^3 C_L\left(\frac{C_L}{C_D}\right)^2$, $\dot{r}_{prod} = \frac{v_\omega \cos(\beta)}{3}$: Reel–out speed
- **Theoretical Power consumed during recovery phase ($\boldsymbol{P_{rec}}$)**

  $P_{rec} = \frac{1}{2}\rho S_{cyl}(v_\omega \cos(\beta) + \dot{r}_{rec})^2 C_{Drec}\dot{r}_{rec}$, $\dot{r}_{rec}$: Reel–in speed
- **Estimated Power produced in one complete cycle ($\boldsymbol{P_{cycle}}$)**

  $$P_{cycle} = \frac{P_{prod}\,\dot{r}_{rec} - P_{rec}\,\dot{r}_{prod}}{\dot{r}_{rec} + \dot{r}_{prod}}$$

➢ Hence, to maximize the power is to maximize the ratio $C_L\left(\frac{C_L}{C_D}\right)^2$, the maximum $C_L\left(\frac{C_L}{C_D}\right)^2$ for the magnus cylinder is found to be at spin ratio, $X = 3.6$.

Control Strategy

Guidance strategy

- We apply the guidance strategy given in [5], and another gain k_η to obtain a constant width trajectory $\eta_{ref} = \frac{k_\eta}{r_t}$.

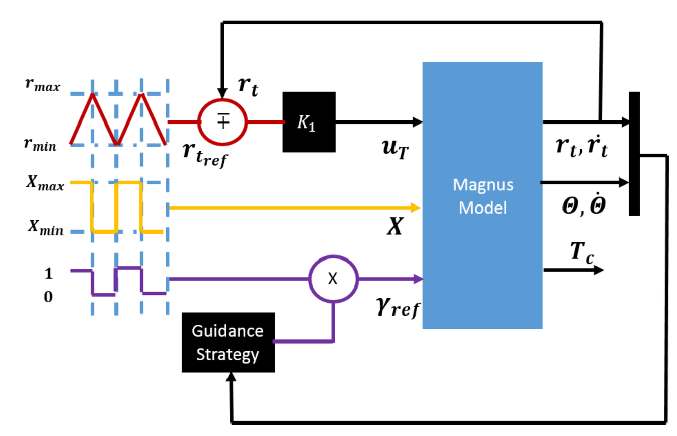

Control of tether length

- A PID controller $\mathbf{K_1}$ is used in order to follow the radial position $\boldsymbol{r_{t_{ref}}}$ through $\boldsymbol{U_T}$ acting on the winch actuator.
- The response time for this control loop is set to be faster than the variations of other forces in order to get an efficient production cycle.

$\boldsymbol{\Theta}$: Attitude of Magnus cylinder by ZYZ $\{\alpha, \delta, \gamma\}$
$\mathbf{T_C}$: Winch Tension
$\boldsymbol{r_t}$: Tether length
$\boldsymbol{\gamma_{ref}}$: Yaw angle in ZYZ transformation
$\mathbf{r_{t_{ref}}}$:Reference radial postion

Simulation Results

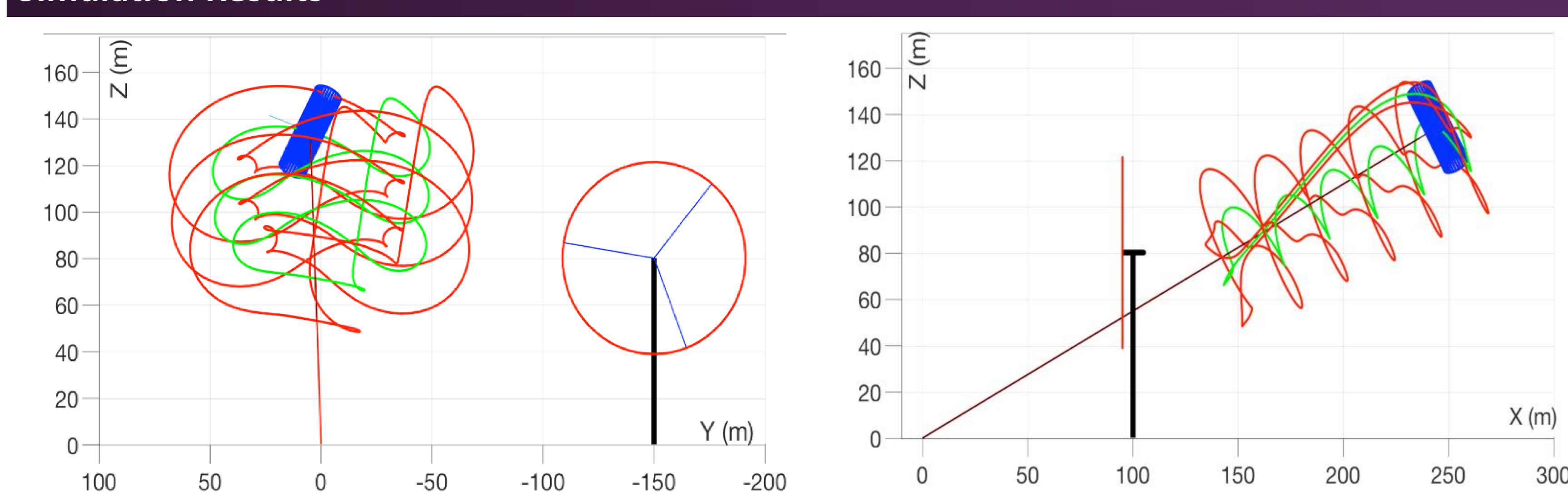

Swept area comparison of a Magnus based AWE system (Surface = 500 m² and Span = 20 m) in a crosswind maneuver with a conventional Wind turbine (1.5 MW).

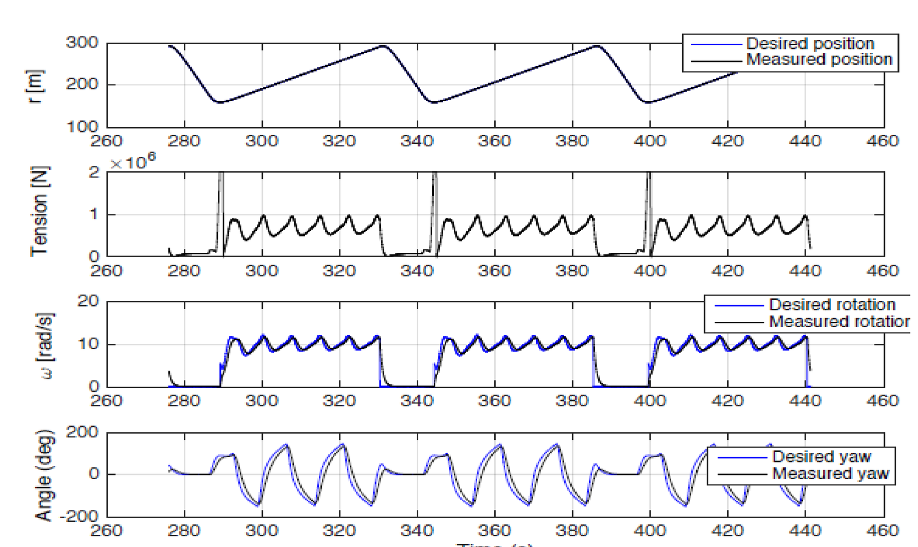

Reference and state variable for tether length ($\boldsymbol{r_t}$, $\boldsymbol{r_{tref}}$), tether tension $\boldsymbol{T_c}$, angular speed of the Magnus rotor ($\boldsymbol{\omega_{cyl}}$, $\boldsymbol{\omega_{cyl_{ref}}}$) , and yaw angle ($\boldsymbol{\gamma}$, $\boldsymbol{\gamma_{ref}}$).

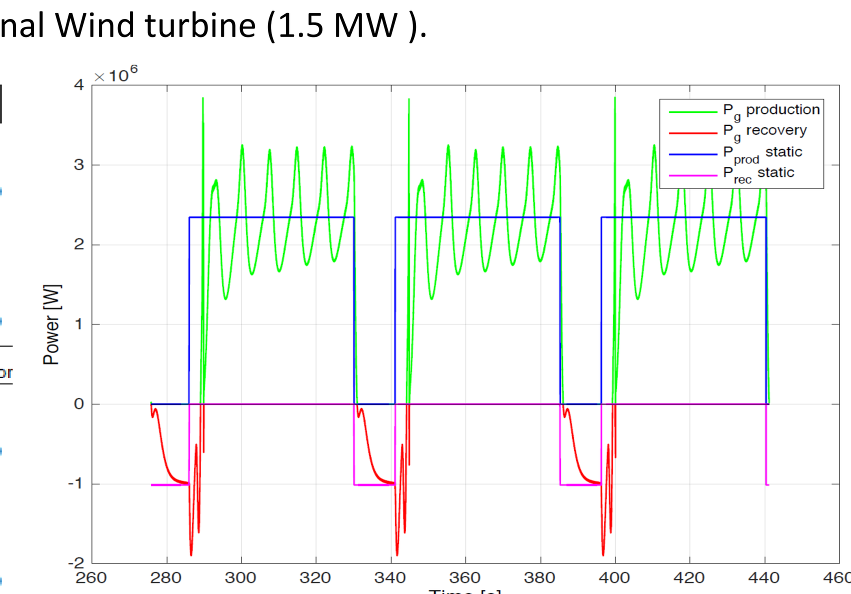

Simulated output power during production and recovery phases with a comparison with a simplified static model $\boldsymbol{P_{static}}$.

Power Curves

Comparision of Power Curve based on static model of a Magnus-based AWE system with that of a conventional Wind turbine (1.5MW).

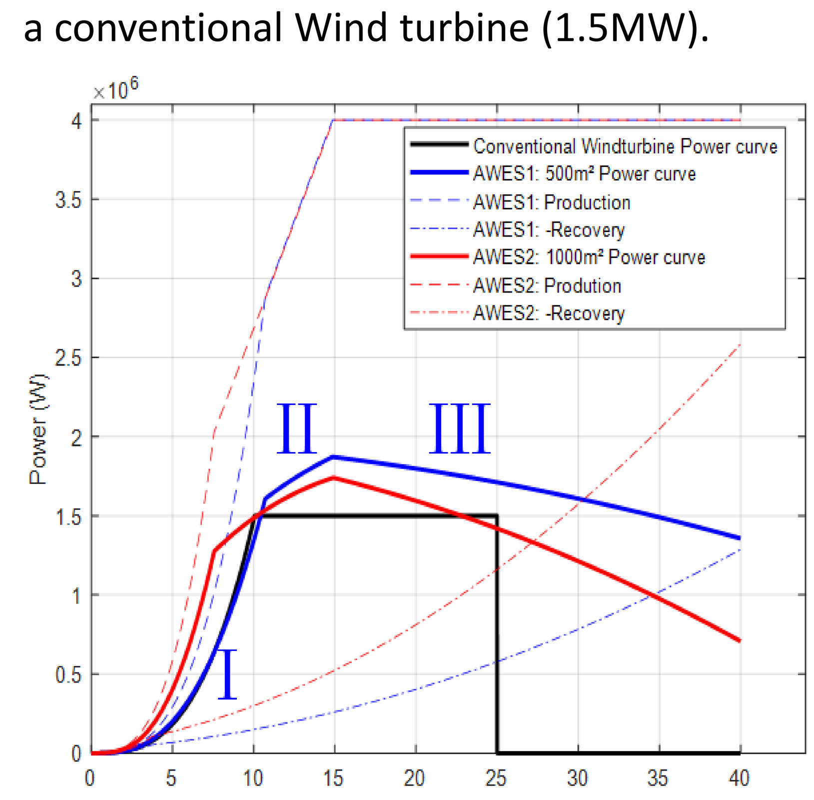

Phase I: Power extraction is maximized following Loyd cond.
Phase II: Maximum traction force is reached, $\dot{r}_{prod}$ continues to increase.
Phase III: Maximum speed of the generator is reached.

By modifying Surface (S_{cyl}), Maximum Tension ($\boldsymbol{T_{max}}$), and Maximum Power($\boldsymbol{P_{max}}$), the shape of the power curve can be adapted according to the distribution of the wind speed at the site.

Conventional Wind turbine : 1.5MW
$\mathbf{AWES_1}$: $S_{cyl} = 500\ m^2, T_{max} = 8e5\ N,\ P_{max} = 4\ MW$
$\mathbf{AWES_2}$: $S_{cyl} = 1000\ m^2, T_{max} = 8e5\ N,\ P_{max} = 4\ MW$

References

[1] Milutinovic´, M., Coric´, M., and Deur, J. (2015). Operating cycle optimization for a Magnus effect based airborne wind energy system. *Energy Conversion and Management*, 90, 154–165. doi: 10.1016/j.enconman.2014.10.066.
[2] Y. Gupta, J. Dumon, and A. Hably, “Modeling and control of a Magnus effect-based airborne wind energy system in crosswind maneuvers,” pp. 1–8.
[3] M. L. Loyd, “Crosswind kite power,” *Journal of Energy*, vol. 4,no. 3, pp. 106–111, 1980.
[4] I. Argatov, P. Rautakorpi, and R. Silvennoinen, “Estimation of the mechanical energy output of the kite wind generator,” *Renewable Energy*, vol. 34, pp. 1525–1532, 2009.
[5] Fagiano, L., Zgraggen, A.U., Morari, M., and Khammash, M. (2014). Automatic crosswind flight of tethered wings for airborne wind energy: modeling, control design and experimental results. IEEE Transactions on Control System Technology, 22(4), 1433–1447. doi: 10.1109/TCST.2013.2279592.